

Texture Enhanced Histogram Equalisation Using TV-L¹ Image Decomposition

Ovidiu Ghita, Dana E. Ilea, and Paul F. Whelan, *Senior Member, IEEE*

Abstract— Histogram transformation defines a class of image processing operations that are widely applied in the implementation of data normalisation algorithms. In this paper we present a new variational approach for image enhancement that has been constructed to alleviate the intensity saturation effects that are introduced by standard contrast enhancement methods based on histogram equalisation. In our work we initially apply total variation (TV) minimisation with a L¹ fidelity term to decompose the input image with respect to cartoon and texture components. Contrary to previous works that rely solely on the information encompassed in the distribution of the intensity information, in our approach the texture information is also employed to emphasize the contribution of the local textural features in the contrast enhancement process. This is achieved by implementing a non-linear histogram warping contrast enhancement strategy that is able to maximise the information content in the transformed image. Our experimental study addressed the contrast enhancement of a wide variety of image data and comparative evaluations are provided to illustrate that our method produces better results than conventional contrast enhancement strategies.

Index Terms—Contrast enhancement, TV-L¹, image decomposition, histogram warping, entropy maximisation.

I. INTRODUCTION

THE optical and sensing limitations that are associated with standard digital image acquisition systems prompted the demand for flexible image processing strategies that are able to maximise the visual transitions between objects that are present in the image data. Thus, among many low-level image processing tasks, the development of automatic contrast enhancement (ACE) strategies forms one distinct direction of research. The main reason behind this considerable interest is motivated by the fact that ACE techniques are often used as precursors to higher level image analysis tasks such as image segmentation, feature extraction and pattern recognition and

their application substantially enhances the performance of the overall computer vision systems. The main principle behind ACE is to accentuate the intensity transitions between the objects captured in the image data and this process usually involves a range of linear or non-linear histogram transformations. More specifically, to maximise the image information, the histogram transformation needs to redistribute the probability of occurrence for each intensity level $i \in M$ (M being the range of intensity values) in the output image to attain a uniform distribution (when the probability for each intensity level in the contrast enhanced image is the same) [1]. Based on this approach, several contrast enhancement (CE) algorithms have been proposed either in the Fourier/wavelet [2,3,4] domain or in the image (spatial) domain [5,6,7,8,9,10,11]. Among these techniques the latter proved more popular when applied to consumer images captured by standard digital cameras, and the major objective resides in the identification of a intensity mapping function $g(\cdot)$ that allows the maximisation of the image contrast: $O_{ij} = g(I_{ij})$, where O is the output (contrast enhanced image), I is the input image and (i,j) denotes the pixel position in the image grid. To achieve contrast enhancement and maintain the appearance of the enhanced image similar to that of the original image, the intensity mapping function $g(\cdot)$ has to be monotonically increasing over the domain K that covers the range of intensity values in the input image I , $K \subseteq M$, where M is the complete range of intensity values (for monochrome images $M=[0,255]$). In this way, a wide spectrum of linear and non-linear functions can be theoretically employed for contrast enhancement where the most simplistic formulations are those that implement contrast stretching and gamma correction. It is useful to note that these basic contrast enhancement approaches return acceptable results only in situations where the intensity domain K is strictly a sub-domain of M , i.e. $K \subset M$. To answer this limitation several related approaches based on random spatial sampling or local statistics have been actively explored [7,12,13,14], but the improvement in contrast enhancement has been obtained at the expense of inserting undesirable intensity artefacts (such as staircase effects) due to abrupt discontinuities in the local image content.

To circumvent the complications associated with the implementation of subjective spatially constrained strategies and the occurrence of staircase effects, the contrast enhancement has been approached as a global histogram warping process, and among many potential implementations

Ovidiu Ghita is with the Centre for Image Processing and Analysis (CIPA), School of Electronic Engineering, Dublin City University, Dublin 9, Ireland (phone: +353-1-7007637; fax: +353-1-7005508; e-mail: ghita@eeng.dcu.ie).

Dana E. Ilea, Paul F. Whelan are with the Centre for Image Processing and Analysis (CIPA), School of Electronic Engineering, Dublin City University, Dublin 9, Ireland (e-mail: danailea@eeng.dcu.ie, paul.whelan@dcu.ie).

the contrast enhancement techniques based on global histogram equalization (GHE) proved most common [6,7,15]. While the application of GHE methods maximises the information content (entropy) in the transformed image, it is important to mention that this global transformation introduces saturation effects and over-enhancement. Alleviation of these problems has attracted substantial research interest and several approaches based on multi-objective optimisation [7], contrast limited adaptive histogram equalisation [16,17,18] and on the adaptive combination of global and local contrast enhancement [19,20] have been intensively explored. In this paper we propose to address the side effects introduced by GHE using a multi-stage TV-L¹ contrast enhancement approach and we will experimentally demonstrate that our approach, as opposed to more conventional GHE techniques, substantially reduces the over-enhancement and the intensity saturation effects. Additional practical advantages that are associated with the proposed contrast enhancement algorithm are also demonstrated in the context of edge detection and cartoon rendering. This paper is organised as follows. Section II briefly review the theoretical and practical issues related to the selection of the histogram transformation for contrast enhancement. In Section III the proposed variational approach for contrast enhancement is introduced, which is followed in Section IV by a detailed analysis of the experimental results. Section V concludes the paper with a summary of the main findings resulting from our study.

II. HISTOGRAM TRANSFORMATION-BASED CONTRAST ENHANCEMENT

The vast majority of contrast enhancement procedures are based on various histogram transformations that attempt to maximise the information content in the input image via intensity mapping. If we assume that the input image is defined as a discrete signal $I_{ij}:\Omega\rightarrow K$, where $\Omega\subset Z^2$ denotes the discrete image domain and $K\subseteq M$ is the domain covered by the intensity values of the pixels in the input image, then the contrast enhancement resides in the identification of the function $g(\cdot)$ that implements the intensity mapping as follows:

$$q = g(s), \quad s \in K, \quad q \in M \quad (1)$$

where $s = I_{ij} | (i, j) \in \Omega$ represents the intensity values of the pixels in the input image and q is the corresponding intensity value in the contrast enhanced image. As indicated in [8] this problem can be formulated as a general variational minimisation model and the intensity mapping function $g(s)$ can be implemented using a family of functions $w(s)$ as follows:

$$g(s) = \frac{L}{\int_0^N w(s) ds} \int_0^s w(r) dr \quad (2)$$

where N and L are the right bounds of the intensity domains K and M , respectively (i.e. $N = \sup(K)$, $L = \sup(M)$). Hence, the contrast enhancement can be reformulated as the problem of finding the function $w(s)$ that is able to maximise the

information content in the output image. In this regard, if we replace $w(s)=1$ in (2) we obtain the standard minimum-maximum intensity stretch operation $g(s) = \frac{L}{N} s$, $s \in [0, N]$ and if we replace $w(s)$ with the histogram of the input image $h(s)$, $s \in [0, N]$ we end up with the standard histogram equalisation process $g(s) = \frac{L}{\text{card}(\Omega)} \int_0^s h(r) dr$ (where $\text{card}(\Omega)$ denotes the cardinality of the image domain Ω where the input image I is defined), which is the most common approach applied for global contrast enhancement. Although many formulations for $w(s)$ can be devised, the use of histogram equalisation in the context of contrast enhancement is motivated by two main reasons. Firstly, the histogram equalisation process redistributes the intensity information in such a way that the inter-histogram bar spacing is minimised. Secondly, this histogram transformation approach is able to (theoretically) maximise the information content in the contrast enhanced image. While these properties are opportune for contrast enhancement, it is important to highlight that histogram equalisation exhibits several limitations such as the incidence of intensity saturation and over-enhancement.

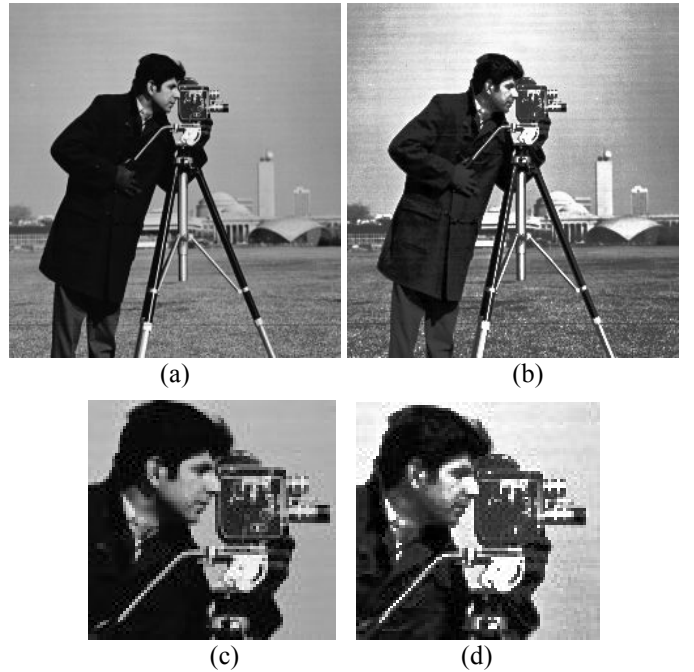


Fig. 1. Global histogram equalisation contrast enhancement. (a) Input image. (b) GHE contrast enhanced image. Close-up details taken from the input (c) and contrast-enhanced (d) images to illustrate the intensity saturation and over-enhancement artefacts that are introduced by the application of the histogram equalisation process.

These problems are clearly illustrated in Fig. 1 where the histogram equalisation process has been applied to the standard ‘‘Cameraman’’ test image. For visualization purposes, close-up details are provided to highlight the intensity artefacts that are introduced during the contrast enhancement process. To redress these undesirable contrast enhancement problems that are introduced by histogram equalisation, in this work we

propose a multi-stage variational-based contrast enhancement algorithm that will be detailed in the next section of the paper.

III. PROPOSED CONTRAST ENHANCEMENT METHOD

The proposed contrast enhancement approach involves a multi-step algorithm that initially applies the TV-L¹ model to attain the cartoon-texture decomposition of the input image. After the extraction of the cartoon-texture image components, contrast enhancement is achieved by applying a non-linear histogram warping process that emphasises the contribution of the texture information in the intensity distribution of the contrast enhanced image. An overview that details the proposed contrast enhancement algorithm is depicted in Fig. 2 and full details about each computational component will be provided in the remainder of this section.

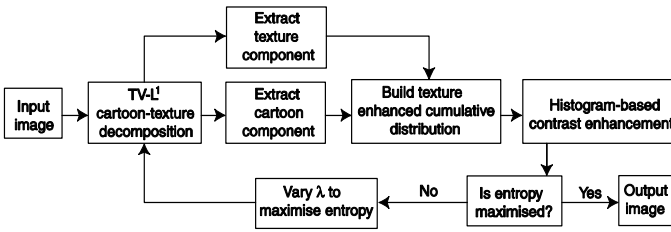


Fig. 2. Overview of the proposed contrast enhancement algorithm.

A. TV-L¹ Cartoon-Texture Decomposition

An important component of the proposed contrast enhancement strategy is represented by the process relating to the cartoon-texture decomposition. The main objective of this process (in the context of the proposed application) is to extract the texture component, as this information emphasises the meaningful patterns contained in the input image and rejects the undesirable intensity transitions that are caused by variations in illumination conditions. The problem of cartoon-texture decomposition can be efficiently solved as a global variational model [21,22,23,24]. Total variation (TV) models have been widely employed for data denoising [25,26,27] and recently have found other interesting applications in the fields of face recognition [20], texture enhancement [28], inpainting [29,30] and blind deconvolution [31]. Using this variational approach, the input image can be decomposed as follows: $I = c + t$, where c and t denote the cartoon and texture components, respectively. The cartoon image c , which contains the de-textured objects (or non-oscillatory components) from the input image I , can be determined by minimising the following expression:

$$\min_c \int_{\Omega} |\nabla c| + \lambda \|I - c\|_{L^1} d\Omega \quad (3)$$

where $\Omega \subset Z^2$ denotes the image domain and the symbol $\|\cdot\|_{L^1}$ defines the L¹ norm. The TV-L¹ model depicted in (3) consists of two distinct terms that are calculated over the image domain Ω . The first term in (3) implements a PDE-based de-texturing process (i.e. the total variation of the cartoon component c), while the second term defines a fidelity term that forces the intensity values in c to remain close to

those in the original image I . The TV-L¹ variational model is controlled by the Lagrange multiplier $\lambda \in R^+$, which is inversely proportional to the strength of the data smoothing process. Using the calculus of variations (see Appendix A) we can derive the Euler-Lagrange equation of (3) and the steady state solution can be iteratively obtained by artificial time discretization as follows:

$$c_t = \nabla \cdot \left(\frac{\nabla c}{|\nabla c|} \right) + \lambda \frac{I - c}{|I - c|}, \quad c(t=0) = I \quad (4)$$

where c_t is the partial derivative of c with respect to the time variable t , $\nabla \cdot$ is the divergence and ∇ denotes the gradient operator. The implementation of (4) in the discrete image domain requires the approximation of the partial derivatives with central differences where the solution is found by the steepest gradient descent as indicated in (5).

$$c_{ij}^{n+1} = c_{ij}^n + \frac{\Delta t}{\Delta x \Delta y} \left(\nabla_x^- \left(\frac{\nabla_x^+ c_{ij}^n}{|\nabla_x c_{ij}^n| + \beta} \right) + \nabla_y^- \left(\frac{\nabla_y^+ c_{ij}^n}{|\nabla_y c_{ij}^n| + \beta} \right) \right) + \Delta t \left(\lambda \frac{I_{ij} - c_{ij}^n}{(I_{ij} - c_{ij}^n)^2 + \varepsilon} \right), \quad s.t. \quad \beta, \varepsilon \rightarrow 0 \quad (5)$$

where (i,j) denotes the position of the pixel in the image, ∇^+ and ∇^- are the forward and backward discrete gradients, respectively, $|\nabla c_{ij}|$ is the magnitude of the gradient, Δt is the time step, n is the iteration index, and Δx and Δy are the discrete spatial distances of the image grid. The expression in (5) implements the mean curvature with the fidelity (constraint) term $\lambda \frac{I - c}{|I - c|}$ and is convergent if the CFL

condition is upheld ($\frac{\Delta t}{\Delta x \Delta y} \leq \alpha |\nabla c|$, $\alpha \in R^+$ [31]). As

mentioned in [22], the TV-L¹ variational model excels when applied to image decomposition and in this process the optimal selection of the parameter $\lambda \in R^+$ plays an important role. While this parameter is usually selected in conjunction with the level of noise present in the image or based on specific geometrical constraints associated with the image decomposition process (for more details refer to [22,31]), in the proposed implementation the optimisation of this parameter will be conducted to maximise the image content (entropy) in the contrast enhanced image. This will be explained later in the paper. In the proposed contrast enhancement algorithm, the TV-L¹ model is applied to perform cartoon-texture decomposition and the cartoon image c_λ is obtained by applying (5) to the input image. If we assume that the input image is noise-free, the texture component can be determined by simply subtracting the cartoon component c_λ from the input image I as follows:

$$t_\lambda = I - c_\lambda, \lambda \in D \quad (6)$$

where D is the interval of variation for the parameter λ , c_λ and t_λ are the cartoon and texture images, respectively, that are obtained for a value $\lambda \in D$. Fig. 3 illustrates the results obtained when the cartoon-texture decomposition is applied to the ‘‘Cameraman’’ image shown in Fig. 1.

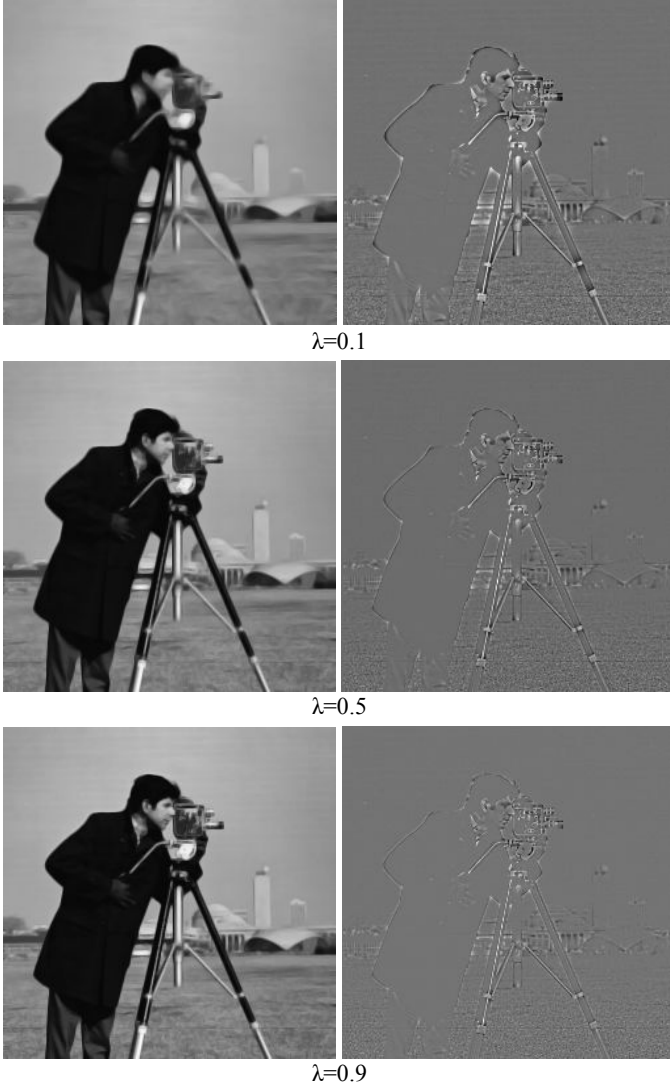


Fig. 3. Cartoon-texture decomposition ($\Delta t = 0.1$) for different values of the parameter λ . Left: Cartoon images. Right: Texture images. Note that the strength of the texture decreases with the increase in the value of λ .

B. Texture-Enhanced Histogram Equalisation

After cartoon-texture decomposition, the next component of the proposed algorithm addresses the calculation of the histogram transformation that is applied for contrast enhancement. As indicated in Section II our aim is to construct a continuous monotonic increasing transformation that is able to avoid the intensity and over-saturation effects that are introduced by the standard histogram equalisation process. The main idea behind this approach is to implement a local intensity mapping process that alters the shape of the histogram calculated from the cartoon image with respect to

the information contained in the texture component. In this regard, the first step is to identify the pixels that are associated with strong textures after the application of the cartoon-texture decomposition. The binary texture map is obtained by applying (7).

$$t_{ij}^b = \begin{cases} 1 & \text{if } |I_{ij} - c_{ij}| > \rho, \rho \in R^+ \\ 0 & \text{Otherwise} \end{cases} \quad (7)$$

where t^b is the binary texture map and ρ is a small positive value. (The parameter ρ controls the strength of the texture information that will be used in the contrast enhancement process and in our implementation ρ has been set to 1.0). Once the identification of the texture pixels that are associated with the input image is finalised, the next step implies the evaluation of the neighbourhood Γ around each texture pixel. Since the neighbourhood Γ encompasses the local texture, which is usually defined by a heterogeneous local distribution, our aim is to identify the extreme intensity values within the neighbourhood Γ that will be used to alter the intensity distribution H_c that is calculated from the cartoon component c_λ . The aim of this histogram transformation is to overemphasise the contribution of the local texture in the calculation of the histogram H_c and the result of this process is illustrated in Fig. 4. As illustrated in Fig. 4, it can be observed that the application of the texture-enhanced histogram transformation generates a more uniform distribution than the distribution calculated from the original (input) image, and this not only allows the preservation of the textural features during the contrast enhancement process, but also avoids the introduction of saturation effects. All operations associated with the proposed texture-enhanced histogram transformation are shown in equation (8) and in the pseudocode sequence depicted in (9).

$$H_c = \bigcup_{p \in M} h_c(p), \quad h_c(p) = \int_{(i,j) \in \Omega} \delta(c_{ij}, p) d\Omega, \quad (8)$$

$$\text{where } \delta(c_{ij}, p) = \begin{cases} 1 & \text{if } c_{ij} = p \\ 0 & \text{if } c_{ij} \neq p \end{cases}$$

Texture-enhanced histogram transformation:

```

for  $\forall (i, j) \in \Omega$ 
  if  $(t_{ij}^b) == 1$ 
    construct  $\Gamma_{i,j}$  and calculate  $l = \inf_{\Gamma_{i,j}}(c_\lambda)$ ,  $h = \sup_{\Gamma_{i,j}}(c_\lambda)$ 
    for  $(p \in [l, h])$ 
       $H_c(p) = H_c(p) + 1$ 
    end
  end
end

```

(9)

where H_c is the intensity distribution (histogram) calculated from the cartoon image c_λ , Ω is the image domain,

$M \subset [0,255]$ defines the intensity domain, t_{ij}^b is a texture pixel at location (i,j) in the image, Γ_{ij} is the 3×3 neighbourhood around t_{ij}^b , $\inf(\cdot)$ and $\sup(\cdot)$ are the infimum and supremum operators, l and h are the lowest and highest intensity values within Γ_{ij} in the cartoon image c_λ .

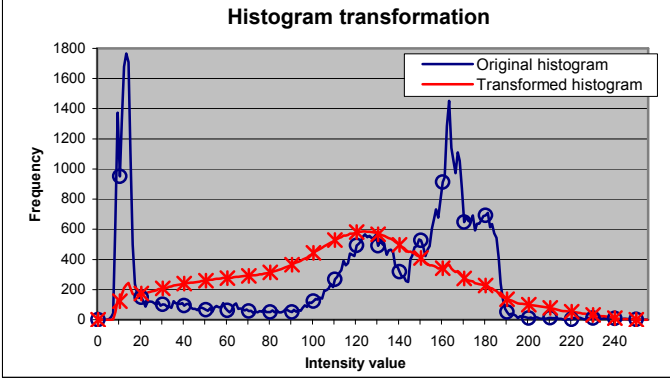


Fig. 4. Texture-enhanced histogram transformation. Note the more uniform distribution of the intensity information in the transformed histogram. Blue-circled line – histogram calculated from the “Cameraman” cartoon image ($\lambda=0.1$) - see Fig. 3. Red-barbed line – transformed histogram.

After the calculation of the texture-enhanced distribution H_c (using 8 and 9), the next step involves the construction of the cumulative distribution $g(s)$ that will be used as a look-up-table in the histogram equalisation process.

$$g(s) = \kappa \int_0^s H_c(r) dr, \quad O_{ij} = g(I_{ij}) | (i, j) \in \Omega \quad (10)$$

where $\kappa = \frac{L}{\int_0^L H_c(r) dr}$, $L = \sup(M)$ is a scaling factor that

maps the intensity transformation within the interval M and $O_{ij} | (i, j) \in \Omega$ is the contrast enhanced image.

C. Parameter Selection

As indicated in Section III.A, the TV- L^1 -based image decomposition is controlled by the parameter $\lambda \in R^+$, which is inversely proportional to the level of smoothing in the cartoon image c_λ . Since the accurate decomposition of the input image into cartoon and texture components plays the central role in the proposed contrast enhancement strategy, the optimisation of the parameter λ should be conducted with the aim of maximising the information content in the contrast enhanced image. Since entropy [32] is a measure of the average information content present in the image, our objective is to maximise the expression of the entropy $E(\cdot)$ shown in (11), when the value of the parameter λ is varied within the range $[0,1]$.

$$E(H_n) = - \sum_{s \in M} H_n(s) \log_2(H_n(s)), \quad \sum_{s \in M} H_n(s) = 1 \quad (11)$$

$$\lambda_{opt} = \arg \max_{\lambda \in [0,1]} [E(H_n^O)] \quad (12)$$

where E is the entropy measure, H_n is the normalised version of the distribution H , i.e. $H_n(s) = \frac{H(s)}{\sum_{r \in M} H(r)}$, λ_{opt} is the value of λ for which the entropy measure is maximised and H_n^O denotes the normalised histogram of the contrast enhanced image $O_{ij} | (i, j) \in \Omega$ (see equation 10).

IV. EXPERIMENTAL RESULTS

In this experimental study we analyse the performance of the proposed algorithm when compared to performances offered by other relevant histogram specification/equalisation contrast enhancement (CE) techniques. In this regard, four representative contrast enhancement algorithms were selected for comparative purposes: conventional global histogram equalisation (GHE) [1], brightness preserving bi-histogram equalisation (BP-BHE) [17], minimum mean brightness error bi-histogram equalisation (MMBE-BHE) [15] and dynamic histogram equalisation (DHE) [18].

Table I. Numerical results obtained by the proposed TV- L^1 TE-HE and other related histogram equalisation (HE)-based contrast enhancement strategies.

Image	Method	Entropy	EPI α
Cameraman image	GHE	6.76	0.533
	BP-BHE	6.79	0.556
	MMBE-BHE	6.75	0.537
	DHE	6.77	0.558
	TV- L^1 TE-HE	6.86	0.779
Berkeley image	GHE	6.69	0.350
	BP-BHE	6.66	0.347
	MMBE-BHE	6.68	0.398
	DHE	6.64	0.531
	TV- L^1 TE-HE	6.70	0.542
Couple image	GHE	6.35	0.259
	BP-BHE	6.37	0.373
	MMBE-BHE	6.29	0.429
	DHE	6.29	0.455
	TV- L^1 TE-HE	6.47	0.475
Kodak image	GHE	6.84	0.378
	BP-BHE	6.86	0.372
	MMBE-BHE	6.81	0.341
	DHE	6.77	0.447
	TV- L^1 TE-HE	6.90	0.581
Aerial image	GHE	6.31	0.562
	BP-BHE	6.28	0.546
	MMBE-BHE	6.26	0.523
	DHE	6.24	0.558
	TV- L^1 TE-HE	6.34	0.574
Lighthouse image	GHE	7.18	0.601
	BP-BHE	7.22	0.641
	MMBE-BHE	7.19	0.623
	DHE	7.16	0.693
	TV- L^1 TE-HE	7.30	0.796

The BP-BHE, MMBE-BHE and DHE contrast enhancement algorithms were designed to circumvent the saturation and over-enhancement effects that are introduced by GHE by partitioning the histogram of the input image into two [15,17] and multiple components [18] prior to the application of the

histogram equalisation process. Since the objectives of the BP-BHE, MMBE-BHE and DHE algorithms are similar to those associated with the proposed variational approach, these contrast enhancement schemes are particularly suitable to be included in this experimental study.

As indicated in Section II, the main objective of this paper is to propose a new CE algorithm based on TV- L^1 texture-enhanced histogram equalisation (TV- L^1 TE-HE). To allow for a direct comparison between the performances obtained by our algorithm and GHE, BP-BHE, MMBE-BHE and DHE contrast enhancement algorithms, the first experiments are conducted on benchmark images ('Cameraman', 'Couple', 'Lighthouse', 'Aerial' and other standard images included in the Kodak and Berkeley databases) and the algorithm performance will be sampled by metrics such as entropy and

edge enhancement. The experimental results depicted in Figs. 5 to 8 augment the numerical data reported in Table I (in this table additional results are also reported for images depicted in Fig. 9) and they illustrate that the proposed algorithm is able to outperform the other CE techniques investigated in this study with respect to the avoidance of intensity saturation and over-enhancement. As indicated earlier, edge enhancement is another metric that is commonly used in the assessment of CE techniques and the results reported in Figs. 10 and 11 show that the proposed algorithm outperforms the GHE, BP-BHE, MMBE-BHE and DHE with respect to both edge localisation and edge enhancement (the edge attenuation generated by MMBE-BHE and the noticeable edge distortions introduced by GHE and BP-BHE can be clearly observed in Fig. 11).

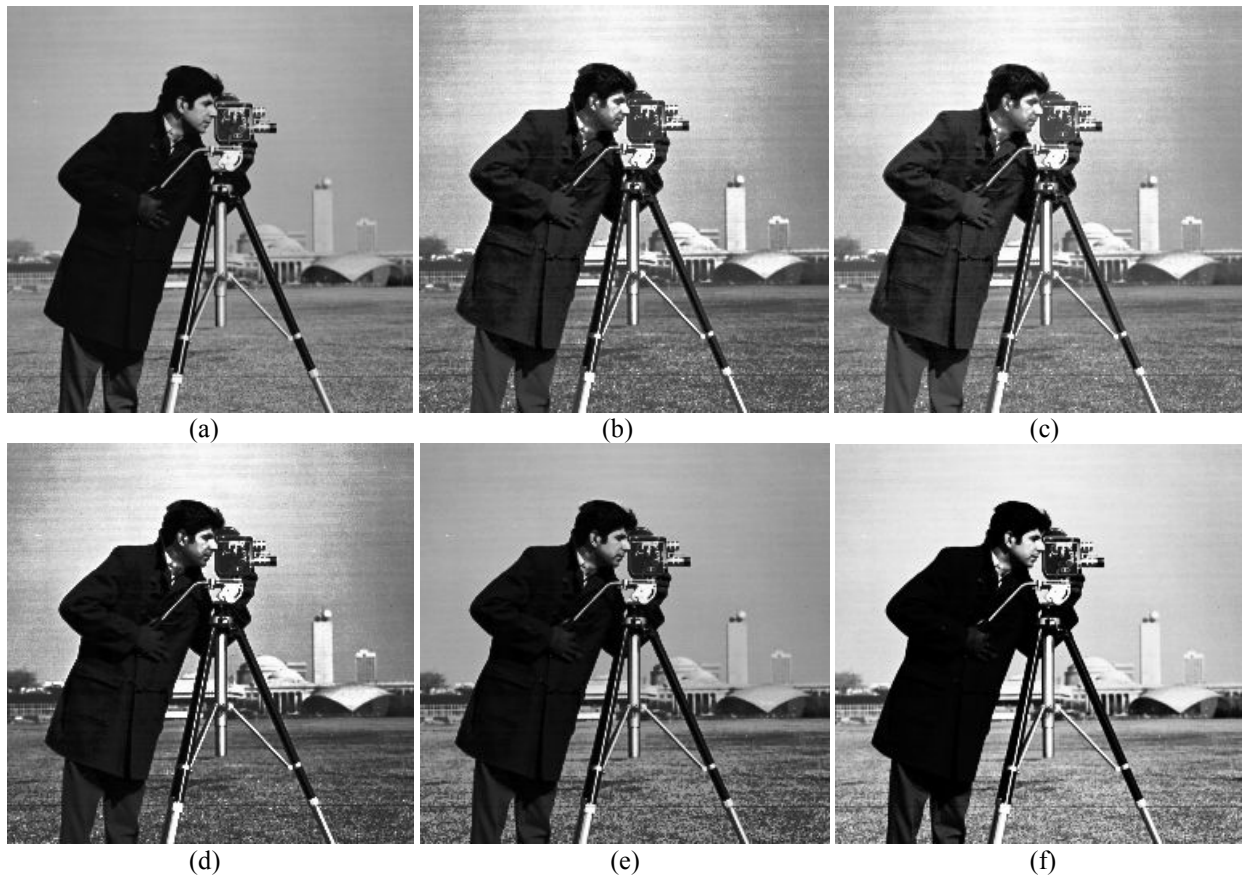


Fig. 5. Contrast enhancement results – 'Cameraman' image. (a) Input image. (b) GHE. (c) BP-BHE. (d) MMBE-BHE. (e) DHE. (f) Proposed TV- L^1 TE-HE.

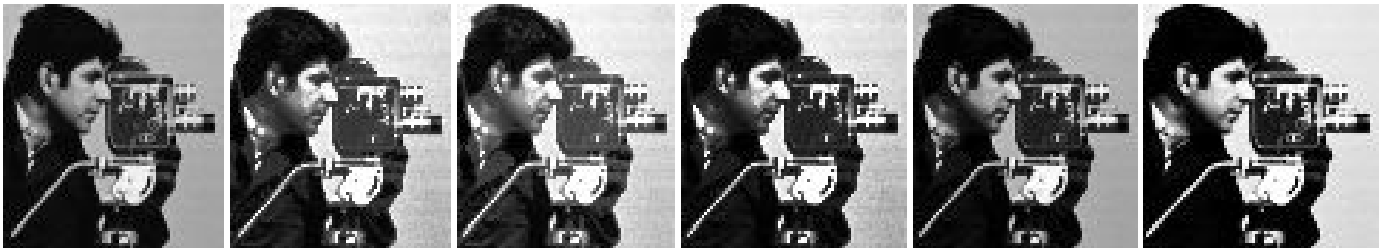


Fig. 6. Close-up details from images depicted in Fig. 5. (Left-right): input image, GHE, BP-BHE, MMBE-BHE, DHE, TV- L^1 TE-HE. Note the avoidance of the intensity saturation effects and over-enhancement that is achieved by the proposed TV- L^1 TE-HE when compared to GHE and other HE-based contrast enhancement strategies.

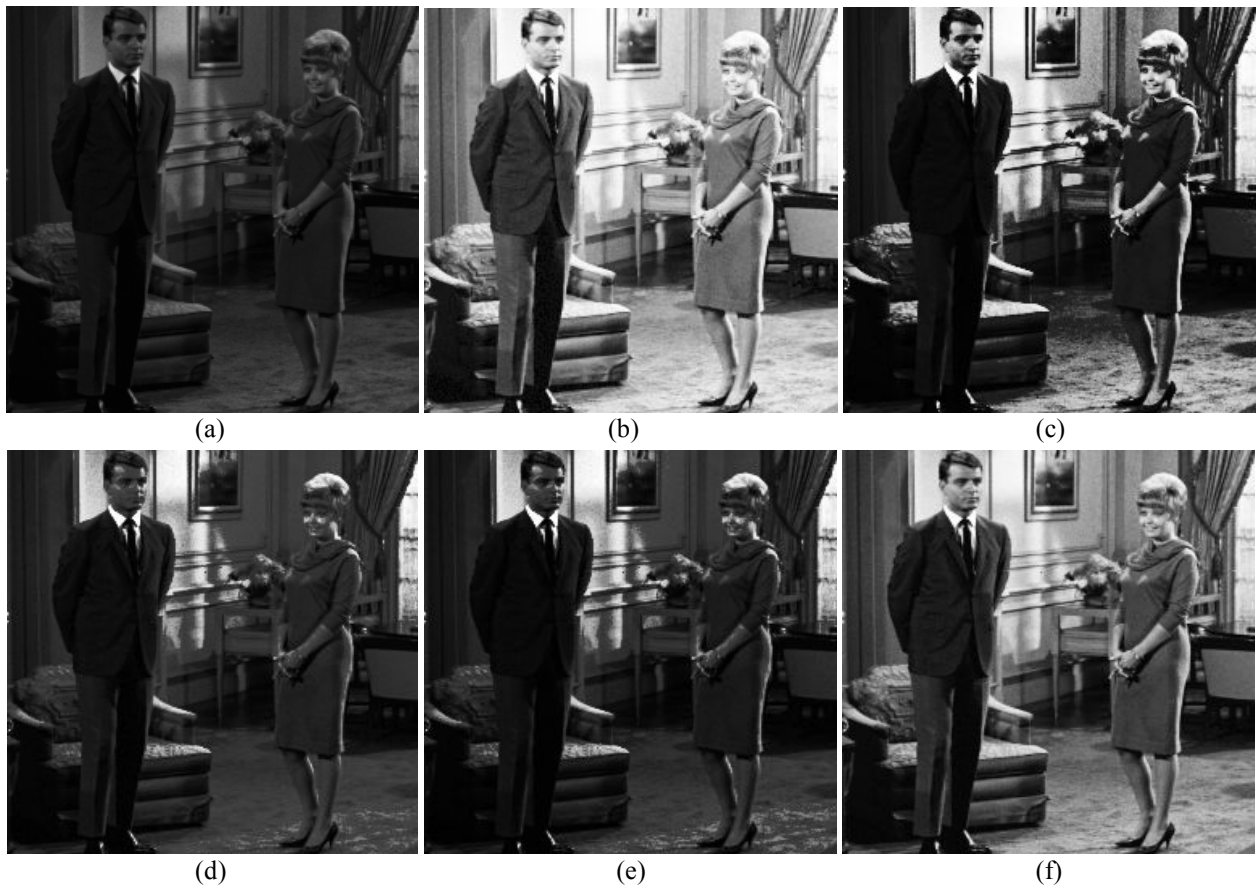


Fig. 7. Contrast enhancement results – ‘Couple’ image. (a) Input image. (b) GHE. (c) BP-BHE. (d) MMBE-BHE. (e) DHE. (f) Proposed TV-L¹ TE-HE.



Fig. 8. Close-up details from images depicted in Fig. 5. (Left-right): input image, GHE, BP-BHE, MMBE-BHE, DHE, TV-L¹ TE-HE. Note the avoidance of the intensity saturation effects and over-enhancement that is achieved by the proposed TV-L¹ TE-HE when compared to GHE and other HE-based contrast enhancement strategies.

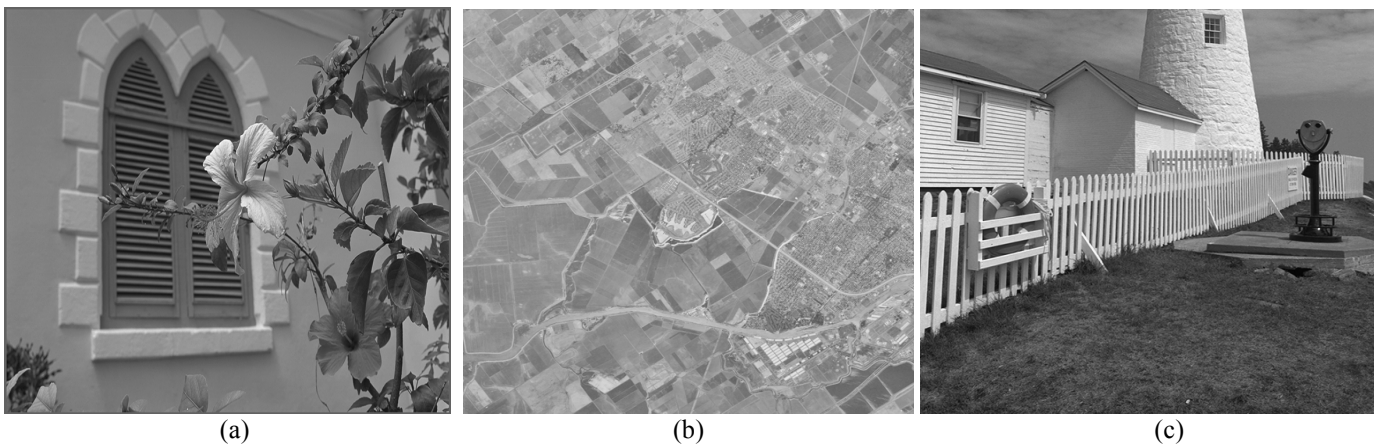


Fig. 9. Additional standard test images used in the experimental evaluation. (a) Kodak database. (b) Aerial image. (c) Lighthouse image.



Fig. 10. Contrast enhancement results – Berkeley database [33] image. (a) Input image. (b) GHE. (c) BP-BHE. (d) MMBE-BHE. (e) DHE. (f) Proposed TV-L¹ TE-HE. Note the crisper edge enhancement obtained by the proposed TV-L¹ TE-HE when compared to GHE and other HE-based contrast enhancement strategies (for additional details please refer to Fig. 8).

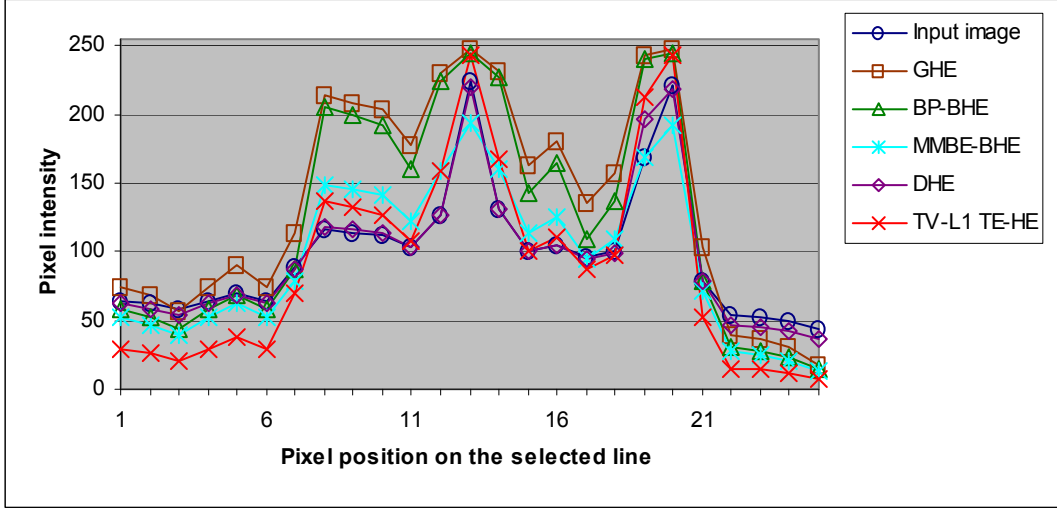


Fig. 11. Edge enhancement – Berkeley database image. Pixel intensities plotted for the highlighted line depicted in image Fig. 10(a).

Another useful aspect associated with the proposed TV-L¹ TE-HE contrast enhancement strategy is its potential to be applied to image data corrupted by noise, as the cartoon-texture decomposition has the ability to reject the noisy signal from the input image data. This useful property can be obtained by simply replacing the input image I in (10) with the cartoon component c_λ that maximises the expression shown in (12). To quantify the improved performance associated with the proposed algorithm we have applied all contrast enhancement schemes that are investigated in this study to the ‘Cameraman’ image that has been corrupted with Gaussian noise (zero mean, standard deviation 10 grey-levels, $\mathcal{N}(0,10)$). Experimental results are presented in Fig. 12 and the efficiency of the contrast enhancement process is validated in the context of edge extraction (see Fig. 13).

To complement the visual results presented in Fig. 13, numerical data are presented in the last column of Table I, where the accuracy of the contrast enhancement is evaluated with respect to edge preservation. In this regard, the contrast enhancement algorithms were applied to image data that has been corrupted with Gaussian noise (zero mean, standard deviation 10 grey-levels, $\mathcal{N}(0,10)$) and the accuracy of the edge preservation is measured with respect to the strength of the edge information in the noiseless image I using the correlation index α that has been suggested in [34].

$$\alpha = \frac{\Lambda(\Delta I - \overline{\Delta I}, \Delta O - \overline{\Delta O})}{\sqrt{\Lambda(\Delta I - \overline{\Delta I}, \Delta I - \overline{\Delta I})\Lambda(\Delta O - \overline{\Delta O}, \Delta O - \overline{\Delta O})}} \quad (13)$$

In (13) Δ is the Laplacian operator, I is the original image, $O = g(I_n)$ is the output image that is obtained after the application of the contrast enhancement to the noisy image $I_n = I + \mathcal{N}(0,10)$, $\overline{\Delta I}$, $\overline{\Delta O}$ are the mean values calculated after the application of the Laplacian operator to images I and O , respectively, and the function $\Lambda(\cdot)$ is defined as follows,

$$\Lambda(\Delta I, \Delta O) = \sum_{(i,j) \in \Omega} \Delta I(i, j) \times \Delta O(i, j) \quad (14)$$

The edge preservation index α takes values in the range [0,1] and the higher its value the more accurate the edge preservation. The edge preservation results reported in Table I indicate that our TV-L¹ TE-HE contrast enhancement algorithm produces better numerical results than the GHE, BP-BHE, MMBE-BHE and DHE contrast enhancement strategies when applied to data corrupted by noise, and they further demonstrate the appropriateness of the cartoon-texture decomposition in the context of contrast enhancement.

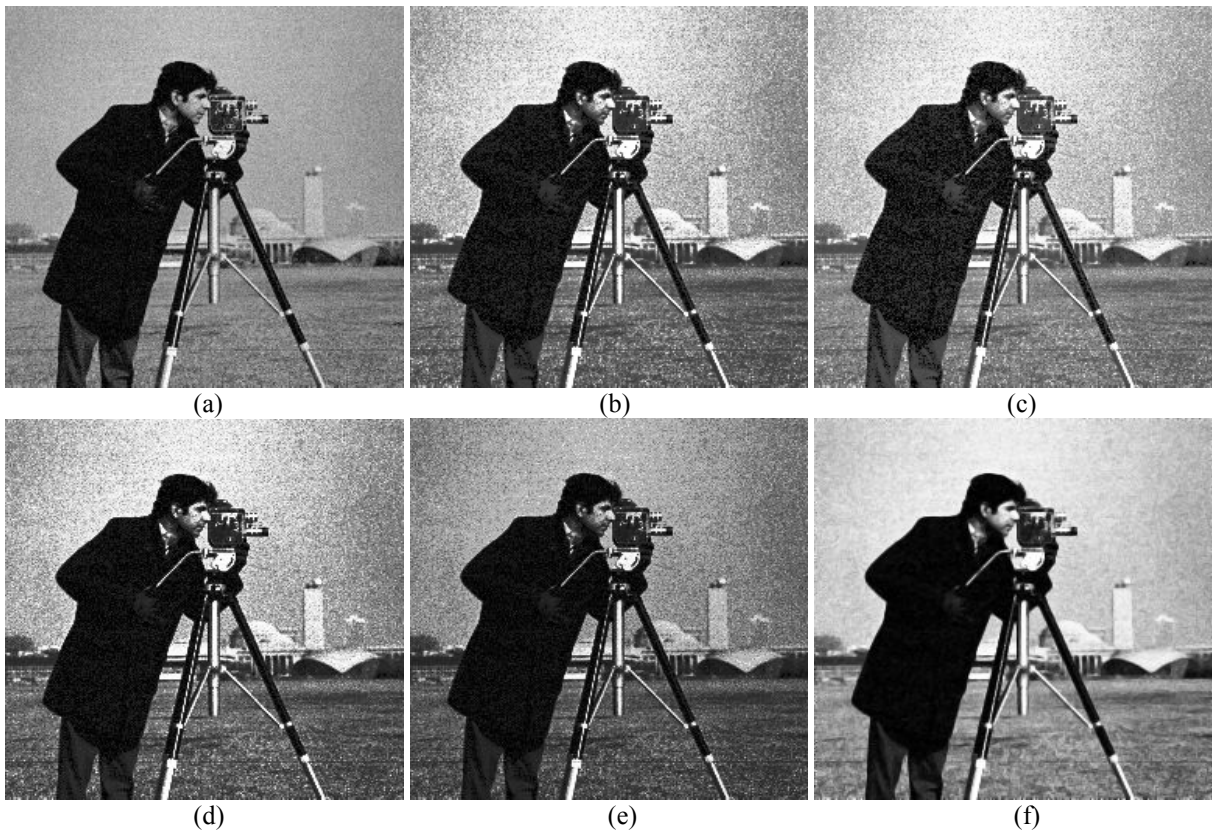


Fig. 12. Contrast enhancement results - 'Cameraman' image corrupted with Gaussian noise, $\mathcal{N}(0,10)$. (a) Input image. (b) GHE. (c) BP-BHE. (d) MMBE-BHE. (e) DHE. (f) TV- L^1 TE-HE.

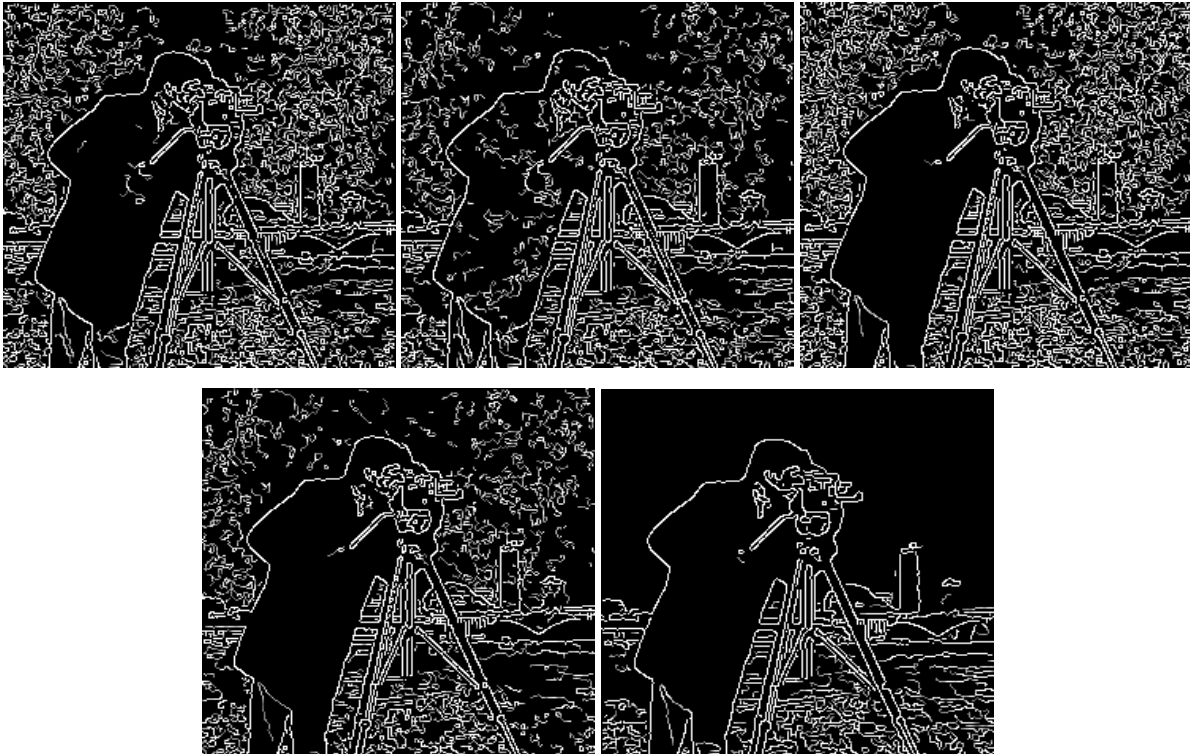


Fig. 13. Edge information extracted using the Canny edge detector corresponding to the images (b-f) shown in Fig. 9.

The last set of results is reported in the context of cartoon rendering of color portrait images. In this regard, we have

applied the cartoon rendering algorithm detailed in [35] to the color contrast enhanced images that are obtained using the

proposed and the HE-based methods (generalisation to color was achieved by converting the input image to the Lab color space and the CE algorithms were applied to the L component) and experimental results are reported in Fig. 14. These additional results clearly indicate that the cartoon rendering in conjunction with the proposed TV-L¹ TE-HE algorithm returns better results (note the more coherent rendering that is achieved in areas defined by skin, which are consistent with the ambient illumination, and the natural enhancement of the highly textured regions such as the eyes and the scarf areas) and they further demonstrate that the inclusion of the proposed contrast enhancement algorithm in the development of more complex image processing tasks leads to improved performance.

V. CONCLUSIONS

The major aim of this paper was to introduce a new variational approach for histogram equalisation which involves the application of the TV-L¹ model to achieve cartoon-texture decomposition. To avoid the occurrence of undesired artefacts such as intensity saturation and over-enhancement that are characteristic for conventional histogram equalisation methods, our approach formulates the histogram transformation as a non-linear histogram warping which has been designed to emphasise the texture features during the image contrast enhancement process. The reported experimental results demonstrate that the proposed TV-L¹ TE-HE strategy is an effective approach for contrast enhancement and they also reveal that the algorithm detailed in this paper offers a flexible formulation that is able to outperform other histogram equalisation-based methods when applied to image data corrupted by noise. Our future studies will focus on the extension of the proposed variational algorithm to attain inter-frame consistent contrast enhancement when applied to low SNR video data and to examine the potential of applying local restoration models that are able to address the image enhancement of medical data that are corrupted by multi-modal noise models.

APPENDIX A

As indicated in Section III.A the cartoon image (or de-textured component) c of the input image I can be obtained by minimising the functional $\Psi(c) = \int_{\Omega} |\nabla c| + \lambda \|I - c\|_{L^1} d\Omega$, where $\lambda \in R^+$ is the Lagrange multiplier, Ω is the image domain and the symbol $\|\cdot\|_{L^1}$ denotes the L¹ norm. The functional $\Psi(c)$ can be re-written in the differential form $F(x, y, c, c_x, c_y) = |\nabla c| + \lambda \|I - c\|_{L^1}$ and its solution can be obtained by applying the Euler-Lagrange equation as illustrated in (A2).

$$\Psi(c) = \iint_{(x,y) \in \Omega} F(x, y, c, c_x, c_y) dx dy \quad (\text{A1})$$

$$\frac{\partial F}{\partial c} - \frac{\partial}{\partial x} \frac{\partial F}{\partial c_x} - \frac{\partial}{\partial y} \frac{\partial F}{\partial c_y} = 0 \quad (\text{A2})$$

where c_x, c_y are the partial derivatives of the cartoon image c (i.e. $c_x = \frac{\partial c}{\partial x}, c_y = \frac{\partial c}{\partial y}$). If we calculate the partial derivatives in (A2) and we consider that $\|I - c\|_{L^1} = |I - c|$ we obtain the following expression:

$$-\lambda \frac{I - c}{|I - c|} - \nabla \cdot \left(\frac{\nabla c}{|\nabla c|} \right) = 0 \quad (\text{A3})$$

This equation approximates the mean curvature flow when $\lambda \in R^+$ [36]. In (A3) the first term implements a fidelity term with respect to the intensity values of the input image I and the second term defines the mean curvature of c ($\nabla \cdot$ denotes the divergence operator). If we assume that the cartoon image c is a function of the time variable t , then the expression shown in (A3) is a first-order Hamilton-Jacobi equation that can be solved using steepest gradient descent,

$$\frac{\partial c}{\partial t} = \nabla \cdot \left(\frac{\nabla c}{|\nabla c|} \right) + \lambda \frac{I - c}{|I - c|} \quad (\text{A4})$$

If we use in (A4) the notation $c_t = \frac{\partial c}{\partial t}$ and we express the mean curvature in terms of the partial derivatives, $\nabla \cdot \left(\frac{\nabla c}{|\nabla c|} \right) =$

$$\frac{\partial}{\partial x} \left(\frac{c_x}{(c_x^2 + c_y^2)^{1/2}} \right) + \frac{\partial}{\partial y} \left(\frac{c_y}{(c_x^2 + c_y^2)^{1/2}} \right), \text{ then (A3) becomes,}$$

$$c_t = \frac{\partial}{\partial x} \left(\frac{c_x}{(c_x^2 + c_y^2)^{1/2}} \right) + \frac{\partial}{\partial y} \left(\frac{c_y}{(c_x^2 + c_y^2)^{1/2}} \right) + \lambda \frac{I - c}{|I - c|} \quad (\text{A5})$$

where the stationary solution for c is obtained for $t \rightarrow \infty$. The implementation of (A5) in the discrete domain is obtained by approximating the partial derivatives $\frac{\partial}{\partial x}, \frac{\partial}{\partial y}, \frac{\partial}{\partial t}$ with central differences as indicated in (5) (see Section III.A).

REFERENCES

- [1] R.C. Gonzalez, R.E. Woods, *Digital Image Processing*, 3rd Edition, Prentice-Hall, 2008.
- [2] A.F. Laine, S. Schuler, J. Fan, W. Huda, "Mammographic feature enhancement by multiscale analysis", *IEEE Transactions on Medical Imaging*, 13(4), 725-740, 1994.
- [3] J.L. Starck, F. Murtagh, E.J. Candès, D.L. Donoho, "Gray and color image contrast enhancement by the curvelet transform", *IEEE Transactions on Image Processing*, 12(6), pp 706-717, 2003.
- [4] Y. Wan, D. Shi, "Joint exact histogram specification and image enhancement through the wavelet transform", *IEEE Transactions on Image Processing*, 16(9), pp. 2245-2250, 2007.
- [5] G. Sapiro, V. Caselles, "Histogram modification via partial differential equations", in *Proc of International Conference on Image Processing (ICIP)*, vol. 3, pp. 632-635, Washington, DC, USA, 1995.



Fig. 14. Cartoon rendering results – Kodak database. (a) Original image. (b) Application of the cartoon rendering algorithm [35] to image (a). (c-g) Application of the cartoon rendering to the image that is contrast enhanced using GHE (c), BP-BHE (d), MMBE-BHE (e), DHE (f) and proposed TV-L¹ TE-HE (g).

- [6] H. Zhu, F.H. Chan, F.K. Lam, "Image contrast enhancement by constrained local histogram equalization", *Computer Vision and Image Understanding*, 73(2), pp. 281-290, 1999.
- [7] N.M. Kwok, Q.P. Ha, D. Liu, G. Fang, "Contrast enhancement and intensity preservation for gray-level images using multiobjective particle swarm optimization", *IEEE Transactions on Automation Science and Engineering*, 6(1), pp. 145-155, 2009.
- [8] I. Altas, J. Louis, J. Belward, "A variational approach to the radiometric enhancement of digital imagery", *IEEE Transactions on Image Processing*, 4(6), pp. 845-849, 1995.
- [9] Y.S. Chiu, F.C. Cheng, S.C. Huang, "Efficient contrast enhancement using adaptive gamma correction and cumulative intensity distribution", in *Proc. of the IEEE International Conference on Systems, Man and Cybernetics*, pp. 2946-2950, Anchorage, USA, 2011.
- [10] M. Grundland, N.A. Dodgson, "Automatic contrast enhancement by histogram warping", *Computational Imaging and Vision*, vol. 32, pp. 293-300, 2004.
- [11] K.S. Sim, C.P. Tso, Y.Y. Tan, "Recursive sub-image histogram equalization applied to gray scale images", *Pattern Recognition Letters*, 28(10), pp. 1209-1221, 2007.
- [12] J.Y. Kim, L.S. Kim, S.H. Hwang, "An advanced contrast enhancement using partially overlapped sub-block histogram equalization", *IEEE Transactions on Circuits and Systems for Video Technology*, 11(4), pp. 475-484, 2001.
- [13] J.A. Stark, "Adaptive image contrast enhancement using generalizations of histogram equalization", *IEEE Transactions on Image Processing*, 9(5), pp. 889-896, 2000.
- [14] W. Kao, M.C. Hsu, Y. Yang, "Local contrast enhancement and adaptive feature extraction for illumination-invariant face recognition", *Pattern Recognition*, 43(5), pp. 1736-1747, 2010.
- [15] S.D. Chen, A. Ramli, "Minimum mean brightness error bi-histogram equalization in contrast enhancement", *IEEE Transactions on Consumer Electronic*, 49(4), pp. 1310-1319, 2003.
- [16] K. Zuiderveld, *Contrast Limited Adaptive Histogram Equalization*, Graphics Gems IV, Academic Press, 1994.
- [17] Y.T. Kim, "Contrast enhancement using brightness preserving bi-histogram equalization", *IEEE Transactions on Consumer Electronic*, 49(1), pp. 1-8, 1997.
- [18] M. Abdullah-Al-Wadud, M.H. Kabir, M.A. Dewan, O. Chae, "A dynamic histogram equalization for image contrast enhancement", *IEEE Transactions on Consumer Electronics*, 53(2), pp. 593-600, 2007.
- [19] T. Jen, B. Hsieh, S. Wang, "Image contrast enhancement based on intensity-pair distribution," in *Proc. of the International Conference on Image Processing (ICIP)*, vol. 1, pp. 913-916, 2005.
- [20] M.H. Kabir, M. Abdullah-Al-Wadud, O. Chae, "Brightness preserving image contrast enhancement using weighted mixture of global and local transformation functions", *International Arab Journal of Information Technology*, 7(4), pp. 403-410, 2010.
- [21] W. Yin, D. Goldfarb, S. Osher, "Image cartoon-texture decomposition and feature selection using the total variation regularized L^1 functional", in *Proc. of Variational, Geometric, and Level Set Methods in Computer Vision (VLSM)*, pp. 73-84, Beijing, China, 2005.
- [22] T. Chen, W. Yin, X.S. Zhou, D. Comaniciu, T.S. Huang, "Total variation models for variable lighting face recognition", *IEEE Transactions on Pattern Analysis and Machine Intelligence*, 28(9), pp. 1519-1524, 2006.
- [23] T.F. Chan, S. Esedoglu, "Aspects of total variation regularized L^1 function approximation", *SIAM Journal on Applied Mathematics*, 65(5), pp. 1817-1837, 2005.
- [24] V. Duval, J.F. Aujol, L.A. Vese, "Mathematical modeling of textures: Application to color image decomposition with a projected gradient algorithm", *Journal of Mathematical Imaging and Vision*, 37(3), pp. 232-248, 2010.
- [25] J.F. Aujol, "Some first-order algorithms for total variation based image restoration", *Journal of Mathematical Imaging and Vision*, 34(3), pp. 307-327, 2009.
- [26] M. Breuß, T. Brox, A. Bürgel, T. Sonar, J. Weickert, "Numerical aspects of TV flow", *Numerical Algorithms*, 41(1), 79-101, 2006.
- [27] O. Ghita, D.E. Ilea, P.F. Whelan, "Image feature enhancement based on the time-controlled total variation flow formulation", *Pattern Recognition Letters*, 30(3), pp. 314-320, 2009.
- [28] O. Ghita, P.F. Whelan, "A new GVF-based image enhancement formulation for use in the presence of mixed noise", *Pattern Recognition*, 43(8), pp. 2646-2658, 2010.
- [29] T. F. Chan and J. Shen, "On the role of the BV image model in image restoration", *Contemporary Mathematics* (Eds. S.Y. Cheng, C.W. Shu, T. Tang), vol. 330, pp. 25-42, 2003.
- [30] S. Esedoglu, J. Shen, "Digital image inpainting by the Mumford-Shah-Euler image model", *European Journal of Applied Mathematics*, vol. 13, pp. 353-370, 2002.
- [31] T.F. Chan, A.M. Yip, F.E. Park, "Simultaneous total variation image inpainting and blind deconvolution", *International Journal of Imaging Systems and Technology*, 15(1), pp. 92-102, 2005.
- [32] C.E. Shannon, "A mathematical theory of communication", *Bell System Technical Journal*, vol. 27, pp. 379-423, 623-656, 1948.
- [33] The Berkeley Segmentation Dataset and Benchmark (BSDB), 2001. http://www.eecs.berkeley.edu/Research/Projects/CS/vision/grouping/seg_bench/
- [34] F. Sattar, L. Florey, G. Salomonsson, and B. Lovstrom, "Image enhancement based on a nonlinear multiscale method", *IEEE Transactions on Image Processing*, 6(6), pp. 888-895, 1997.
- [35] C.I. Larnder, "Augmented perception via cartoon rendering: reflections on a real-time video-to-cartoon system", *ACM SIGGRAPH Computer Graphics*, 40(3), pp. 8:1-8, 2006.
- [36] G. Sapiro, *Geometric Partial Differential Equations and Image Analysis*, Cambridge University Press, ISBN: 9780521790758, 2001.

Ovidiu Ghita received the BE and ME degrees in Electrical Engineering from Transilvania University, Brasov, Romania and the Ph.D. degree from Dublin City University, Ireland. From 1994 to 1996 he was an Assistant Lecturer in the Department of Electrical Engineering at Transilvania University. Since then he has been a member of the Vision Systems Group (VSG) at Dublin City University (DCU) and currently he holds a position of DCU-Research Fellow. Dr. Ghita has authored and co-authored over 90 peer-reviewed research papers in areas of instrumentation, range acquisition, machine vision, texture analysis and medical imaging.

Dana E. Ilea received her B.Eng. degree (2005) in Electronic Engineering and Computers Science from Transilvania University, Brasov, Romania and her Ph.D. degree (2008) in Computer Vision from Dublin City University, Dublin, Ireland. Since 2008 she holds the position of Post Doctoral Researcher within the Centre for Image Processing & Analysis (CIPA), Dublin City University. Her main research interests are in the areas of image processing, texture and colour analysis and medical imaging.

Paul F. Whelan (S'84-M'85-SM'01) received his B.Eng. (Hons) degree from NIHED, M.Eng. degree from the University of Limerick, and his Ph.D. (Computer Vision) from Cardiff University, UK. During the period 1985-1990 he was employed by Industrial and Scientific Imaging Ltd and later Westinghouse (WESL), where he was involved in the research and development of high-speed computer vision systems. He was appointed to the School of Electronic Engineering, Dublin City University (DCU) in 1990 and is currently Professor of Computer Vision (Personal Chair). Prof. Whelan founded the Vision Systems Group (VSG) in 1990 and the Centre for Image Processing & Analysis (CIPA) in 2006 and currently serves as its director.

As well as publishing over 150 peer reviewed papers, Prof. Whelan has co-authored 2 monographs and co-edited 3 books. His research interests include image segmentation, and its associated quantitative analysis with applications in computer/machine vision and medical imaging. He is a Senior Member of the IEEE, a Chartered Engineer and a fellow of the IET and IAPR. He served as a member of the governing board (1998-2007) of the *International Association for Pattern Recognition* (IAPR), a member of the *International Federation of Classification Societies* (IFCS) council and President (1998-2007) of the *Irish Pattern Recognition and Classification Society* (IPRCS). Prof. Whelan is a HEA-PRTL (RINCE, NBIP) and Enterprise Ireland funded principal investigator.